IJIE Int. J. Indust. Entomol. 27(2) 303-311 (2013)
ISSN 1598-3579, http://dx.doi.org/10.7852/ijie.2013.27.2.303

Growth and Osteoblastic Differentiation of Mesenchymal Stem Cells on Silk Scaffolds

Hee-Yeon Cho[1]*, Young-Ae Baik[1]*, Suyeon Jeon[1], Yoon-Hae Kwak[2], Hae Yong Kweon[3], You Young Jo[3], Kwang Gill Lee[3], Young Hwan Park[4], and Dongchul Kang[1]*

[1]*Ilsong Institute of Life Science, Hallym University, Anyang, 431-060, Republic of Korea*
[2]*Department of Orthopaedic Surgery, Hallym University Sacred Heart Hospital, College of Medicine, Hallym University, Anyang, 431-070, Republic of Korea*
[3]*Department of Agricultural Biology, National Academy of Agricultural Science, Rural Development Administration, Suwon, 441-100, Republic of Korea*
[4]*Department of Biosystems and Biomaterials Science and Engineering, Seoul National University, Seoul 151-921, Republic of Korea*

Abstract

In this study, we compared the efficiency of osteoblast differentiation media (ODM) containing three distinct reagent combinations in osteoblastic differentiation of human bone marrow-derived mesenchymal stem cells (hBMSCs) in monolayer culture. In addition, we analyzed growth and differentiation of hBMSCs on silk scaffolds and examined the bone-forming activity of a nanofibrous silk scaffold in a tibia diaphysis defect model of a rat hind limb with intramedullary nailing. Although all three ODM increased alkaline phosphatase activity to a comparable extent, the ODM containing bone morphogenetic protein-2 (BMP-2) was found to be significantly less effective in promoting mineral deposition than the others. Growth of hBMSCs on sponge-form silk scaffolds was faster than on nanofibrous ones, while osteoblastic differentiation was apparent in the cells grown on either type of scaffold. By contrast, bone formation was observed only at the edge of the nanofibrous scaffold implanted in the tibia diaphysis defect, suggesting that use of the silk scaffold alone is not sufficient for the reconstitution of the long bone defect. Since silk scaffolds can support cell growth and differentiation in vitro, loading MSCs on scaffolds might be necessary to improve the bone-forming activity of the scaffold in the long bone defect model.

Int. J. Indust. Entomol. 27(2), 303-311 (2013)

Received : 10 Dec 2013
Accepted : 16 Dec 2013

Keywords:
Silk fibroin,
Mesenchymal stem cell,
Osteoblastic
differentiation

Introduction

Surgical interventions including iliac autograft and allograft are necessary to reconstitute large bone defects resulting from trauma, age-associated bone loss, and occasionally, primary and secondary cancers (Zimmermann and Moghaddam, 2011). However, the supply of bone graft is limited by donor site morbidity for autograft and a shortage of natural resources for allografts. Bone tissue engineering and synthetic bone substitutes have been developed to cope with the clinical demands (Amini

***Corresponding author.**
Dongchul Kang, Ph. D.
Ilsong Institute of Life Science, Hallym University, 1605-4, Ilsong Building 606, Kwanyang-dong, Dongan-gu, Anyang, Kyonggi-do, 431-060, Republic of Korea
Tel: +82-31-380-1868 / FAX: +
E-mail: dckang@hallym.ac.kr

et al., 2012). Bone tissue engineering provides osteoinductive and/or osteoconductive materials to promote natural healing of bone defects and to produce artificial bone substitutes (Schroeder and Mosheiff, 2011). Cells, biomaterials, and regulatory signals are considered to be the three key components in bone tissue engineering (Drosse *et al*., 2008).

Silk fibroin has been used as a suture material for a long time . Silk fibroin is a natural product with well-known biocompatibility and versatile processibility, which renders it widely applicable for tissue engineering (Vepari and Kaplan, 2007). In addition to its utility in textiles and surgical sutures, silk has been used as a biomaterial for tissue engineering of bone, tendon, eardrum, neural conduits, and blood vessels as three-dimensional (3-D) scaffolds, powders, films, and tubes (Kasoju and Bora, 2012). Three-dimensional silk scaffolds fabricated with silk fibroin alone or silk composites with diverse biomaterials and minerals have been employed in bone tissue engineering and are shown to be osteoinductive and osteoconductive in numerous cases including calvarial defect models (Park *et al*., 2010; Zhang *et al*., 2010). Silk scaffolds loaded with various cells and growth factors have also recently been tested in bone tissue engineering (Kirker-Head *et al*., 2007; Meinel *et al*., 2005).

Mesenchymal stem cells (MSCs) can be differentiated into osteoblasts, chondrocytes, adipocytes, myoblasts, and neuronal cells (Dimarino *et al*., 2013). MSCs have been widely used as a cell source for bone tissue engineering (Wang *et al*., 2013). MSC-loaded scaffolds are implanted into bone defects to promote bone regeneration in vivo (Gamie *et al*., 2012). Alternatively, differentiation of MSCs loaded on scaffolds for the production of a bioengineered transplantable bone tissue has been attempted (Hofmann *et al*., 2013; Meinel *et al*., 2005). An MSC-scaffold complex develops bone tissue more efficiently than the scaffold itself at a critical defect of the femoral condyle (Cao *et al*., 2012). The bone-reconstituting capacity of MSC-loaded silk or silk composite scaffolds has also been examined in various experimental settings, which again underscores that MSCs can be used for bone tissue engineering (Wang *et al*., 2006).

MSCs differentiate into osteoblasts in response to combinatorial treatments using dexamethasone (DEX), ascorbic acid (AA) and β-glycerophosphate (βG) with or without BMPs in vitro (Kim *et al*., 2008; Pittenger *et al*., 1999; Wolfe *et al*., 2008). However, diverse combinations of the reagents are being tested for osteoblastic differentiation of MSCs in vitro. In this study, the differentiation efficiency of three distinct combinations of the reagents in ODM was directly compared for growth and differentiation of hBMSCs in monolayer culture. In addition, we analyzed the growth and differentiation of hBMSCs on different silk 3-D scaffolds and examined the bone-forming activity of a 3-D silk scaffold in a tibia diaphysis defect model of a rat hind limb by an intramedullary nailing procedure that is widely used to fix tibia fractures in humans.

Materials and methods

Preparation of silk scaffolds

A silkworm cocoon , harvested from Rural Development Administration (Suwon, Korea), was used for the experiments. The cocoon was sliced and degummed twice with 0.5% on the weight of cocoon (o.w.c.) Marseilles soap and 0.3% o.w.c. sodium carbonate solution at boiling temperature for 1 h and then washed with distilled water. The degummed cocoon was dissolved in $CaCl_2$:H_2O:ethanol (1:8:2). The silk fibroin (SF) solution was obtained after dialysis against distilled water for 4 d and then stored in a refrigerator until use (Kweon *et al*., 2011). All chemicals were used as received without any further purification.

Fibroin solutions (9% w/w concentrations) were obtained by concentrating the above fibroin solution. These solutions together with porogen (300–500 μm NaCl particles) were put into glass disks and then frozen in a −70°C freezer for 12 h to fabricate sponge-type scaffolds 85-1 and 88-1. The composites were lyophilized and then immersed in ethanol and water to induce crystallization and to remove porogen.

Nanofibrous 3-D scaffolds were fabricated by electrospinning of 12% w/w dope solution. The dope was prepared and electrospun into a metal bath filled with methanol as a collector for SF nanofiber as described in Ki *et al*. (2008). Porous nanofibrous scaffolds were prepared by mixing the electrospun SF nanofiber dispersion with NaCl particles of 100–200 μm and 300–500 μm as porogens for scaffolds 1020 and 3050, respectively (Ki *et al*., 2008; Park *et al*., 2010). A glass vessel (φ 6 mm) was filled with the nanofiber dispersion

containing NaCl particles and lyophilized. After cross-linking with glutaraldehyde vapor and subsequent neutralization of the glutaraldehyde with 0.1 M glycine in 0.2 M Na_2CO_3 buffer (pH 9.2), the nanofibrous foam was washed with PBS several times, lyophilized again, and cut into disks (φ 6 mm × 3 mm thick).

Cell culture

hBMSCs (ScienCell Research Laboratories, Carlsbad, CA) were grown in αMEM (Invitrogen, Carlsbad, CA) supplemented with 16.5% fetal bovine serum (Lonza, Basel, Switzerland), 100 units/mL penicillin, and 100 μg/mL streptomycin (JBI, Korea) at 37°C in a humidified 5% CO_2 incubator. hBMSCs at ~80% confluency were subcultured by trypsinization and plating 5 × 10^5 cells on a 10-cm culture dish every 3–4 d.

Osteoblastic differentiation of hBMSCs

Osteoblastic differentiation of hBMSCs was carried out either in a 96-well plate or on the silk scaffolds. hBMSCs up to passage 10 were plated at 8,000 cells/well in a 96-well plate and treated with ODM on the next day. Alternatively, hBMSCs (5×10^4) inoculated on a silk scaffold (φ 6 mm × 3 mm thick for 10/20 and 30/50 or a quarter of φ 9 mm diameter × 1.5 mm thick for 85-1 and 88-1) were grown for a week before treatment with ODM. Three different combinations of dexamethasone (DEX), ascorbic acid (AA), and β-glycerophosphate (βG) were used for osteoblastic differentiation of hBMSCs, namely, ODM 1–50 μM AA, 10 mM βG, 100 nM DEX (Pittenger *et al*., 1999); ODM 2–50 μg AA, 10 mM βG, 100 nM DEX, 100 ng/mL BMP-2 (Kim *et al*., 2008); and ODM 3–100 μM AA, 20 mM βG, 10 nM DEX (Wolfe *et al*., 2008). ODM was refreshed every 3–4 d for up to 2 wk.

MTT assay

The viability of hBMSCs seeded in a 96-well plate at 8,000 cells/well was measured by methylthiazolyldiphenyl-tetrazolium bromide (MTT; Sigma-Aldrich, St Louis, MO, USA) assay as described in Huynh *et al*. (2011). The MTT assay was modified from the 96-well plate protocol to monitor hBMSC viability in a silk scaffold (inoculated at 5×10^4 cells in the same dimension as above). Briefly, the cell-containing scaffold was incubated with 0.5 mL of 0.5 mg/mL MTT solution for 3 h at 37°C. An equal amount of formazan solubilizer (10% SDS in 0.01N HCl) was added and incubated at 37°C overnight. An aliquot (200 μL) of solubilized formazan was transferred to a 96-well plate, and the absorbance at 570 nm, with the reference absorbance at 650 nm, was measured with a Multiskan GO Spectrophotometer (Thermo Scientific, Rockland, IL, USA).

Alkaline phosphatase assay

Alkaline phosphatase (ALP) activity was measured directly for each well in a 96-well plate (Kim *et al*., 2009). After the medium was aspirated out, a 150-μL ALP reaction mixture containing 140 μL of alkaline buffer (Sigma-Aldrich) and 10 μL substrate solution (0.225 M *p*-nitrophenyl phosphate and 1.5 mM $MgCl_2$) was added directly to each well. The reaction was stopped by transferring a 20-μL fraction of the reaction to 80 μL 0.2N NaOH pre-aliquoted in a 96-well plate. Absorbance at 405 nm was measured with a Multiskan GO Spectrophotometer. ALP activity was normalized with viable cell amount measured by the MTT assay.

Alizarin S and von Kossa staining

Cells in a 96-well plate and in a silk scaffold were fixed with PBS-buffered 10% formalin for 30 min at RT. After washing with distilled water twice, the plate and scaffold were incubated in 1% Alizarin S solution or 5% silver nitrate for 30 min at RT. Then, they were washed with distilled water and dried in air. Stained Alizarin S was eluted by incubation in 100 μL of 100 mM cetylpyridinium chloride for 1 h and quantified by measuring absorbance of the eluate at 570 nm with a Multiskan GO Spectrophotometer. Cells grown in a silk scaffold were visualized by staining with 1 μg of 4′,6′-diamidino-2-phenylindole (DAPI)/mL PBS after permeabilization with 0.2% Triton X-100.

In vivo bone formation assay

The in vivo-bone reconstitution capacity of a nanofibrous silk 3-D scaffold 3050 was assessed by implanting the scaffold into a rat tibia diaphysis defect. The tibia of the right hind limb

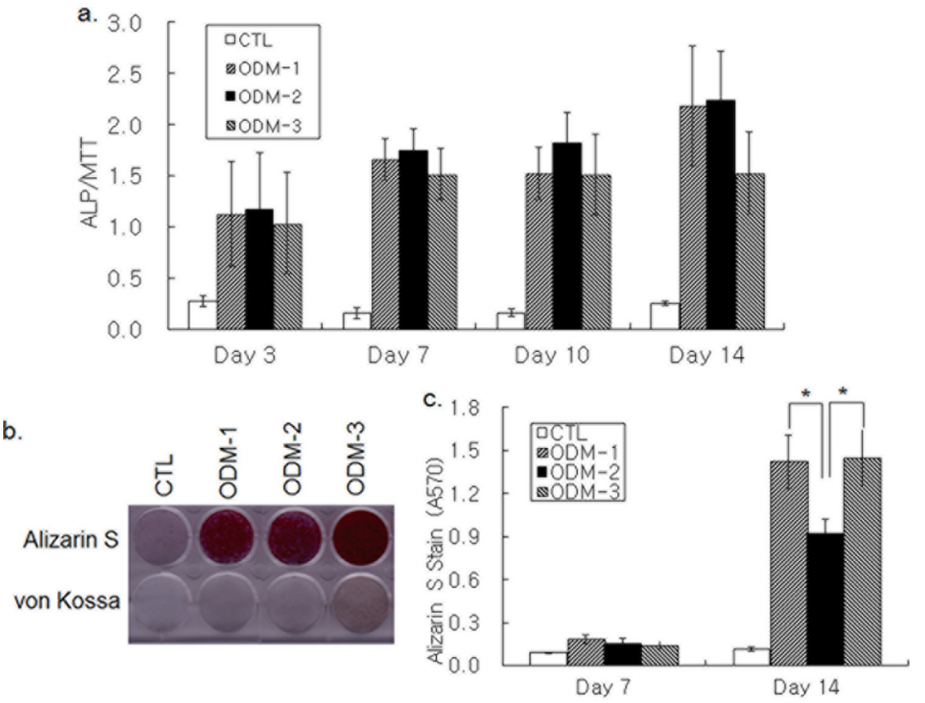

Fig. 1. Osteoblastic differentiation of hBMSCs by three ODM with distinct combinations of DEX, AA, βG, and BMP-2. **a.** ALP activity of hBMSCs on indicated days after treatment of ODM-1, 2, and 3. ALP activity was normalized against the MTT value to compensate cell number variation. Results shown are average ± standard error of five experiments. **b.** Alizarin S and von Kossa staining of differentiation-induced hBMSCs by treatment with the indicated ODM for 14 d. **c.** Intensity of Alizarin S staining. Absorbance at 570 nm of cetylpyridinium chloride-extracted Alizarin S was measured to determine intensity of Alizarin S deposited by differentiating hBMSCs. Results shown are average ± standard error of seven experiments. * depicts $p < 0.05$.

of a rat (~350 gm male Sprague Dawley, RaonBio, Korea) anesthetized by inhalation of isoflurane (Hana Pham Co., Ltd, Korea) was exposed, and a ~3 mm longitudinal defect was generated by a sagittal saw (INT-200S, INTEC). An intramedullary nail (φ 0.9~1.2 mm, Solco Biomedical, Korea) loaded with the silk scaffold (3050) was installed into the tibia defect to fill the gap. Then, the site of surgery was closed with a black silk suture (Ailee Co., Ltd., Korea), and ceftriaxone (4 mg in 100 μL) was injected intradermally for prophylactic purpose. Bone formation was monitored weekly by radiography with EZX-60 portable dental X-ray (Genoray Co., Ltd., Korea). Animal care and operating procedures were approved by the Hallym University Medical Center Institutional Animal Care and Use Committee, Korea (HMC2012-0-1026-1).

H & E and Masson trichome stain

Nine wks post operation, the lower limb was surgically extirpated, and soft tissue was removed with a scalpel. After removal of the intramedullary nail, the tibia was decalcified by incubation in Calci-clear Rapid (National Diagnostics, Atlanta, GA) at room temperature overnight. Paraffin-embedded tissue was processed by the standard procedure of hematoxylin and eosin (H & E) staining. Masson trichrome staining was carried out with the Trichrome Stain Kit (Sigma-Aldrich) according to the manufacturer's protocol.

Results

Osteoblastic differentiation of hBMSCs

Osteoblastic differentiation was induced by treatment of hBMSCs grown in 96-well plates with three different combinations of DEX, AA, βG, and BMP-2. ALP activity was increased in 3 d of ODM treatment and kept increasing until

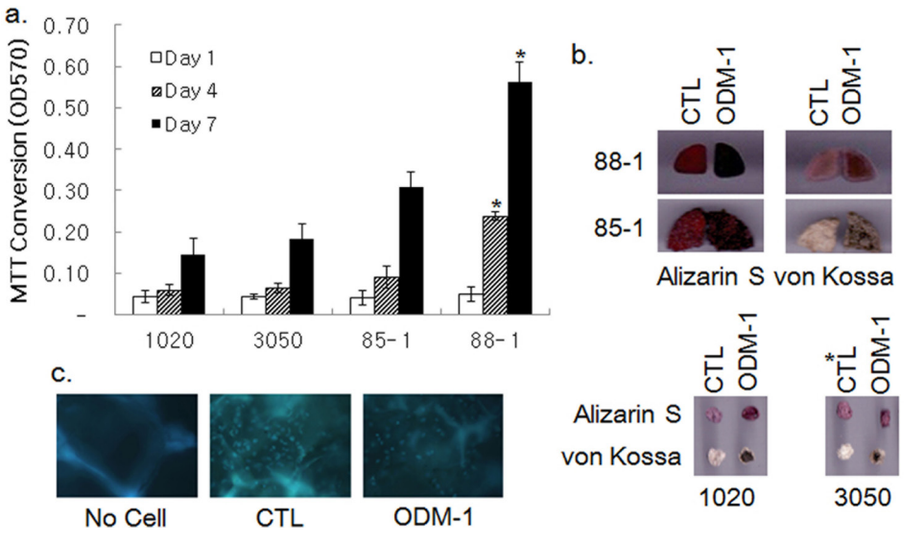

Fig. 2. Growth and differentiation of hBMSC on silk 3-D scaffolds. **a.** MTT assay results for cells grown on specified silk 3-D scaffolds for the indicated periods. Results shown are average ± standard error of three experiments. * depicts $p < 0.05$. **b.** Differentiation of hBMSC grown on silk 3-D scaffolds. Alizarin S and von Kossa staining results of silk 3-D scaffolds loaded with hBMSC. Osteoblastic differentiation of hBMSCs grown on the silk scaffolds was induced by ODM-1 treatment. **c.** DAPI staining of cells grown and differentiated on a silk scaffold. Silk scaffolds 88-1 with differentiated hBMSC were stained with DAPI after fixation and permeabilization, and were observed with a LSM 510 confocal microscope (Carl Zeiss, Oberkochen, Germany).

d 14 (Fig. 1a). Although the ALP activity increase on d 14 by ODM-3 appeared lower than that by ODM-1 and ODM-2, the difference was not significant statistically. Deposition of bone mineral by differentiating hBMSCs was determined by Alizarin S and von Kossa staining. An increase in both Alizarin S and von Kossa staining was not apparent in 7 d, but all three differentiation media increased the staining intensity strongly on d 14 (Fig. 1b). Colorimetric measure of Alizarin S precipitate showed that Alizarin S staining was stronger in the ODM-1 and ODM-3-treated groups than in the ODM-2-treated one, suggesting that ODM-2 was less efficient for calcium deposition than ODM-1 and ODM-3 (Fig. 1c). Moreover, the intensity of von Kossa staining was the strongest with ODM-3 treatment (Fig. 1b). In summary, although all three differentiation media tested were similarly effective in ALP activity increase, there was a significant difference in their potencies to induce mineral deposition.

Growth of hBMSC and osteoblastic differentiation on silk scaffolds

The growth of hBMSCs in various silk 3-D scaffolds was examined by MTT assay. Fibroin nanofibrous scaffolds with pores of φ 100–200 (1020) and 300–500 (3050) μm, and two sponge-type scaffolds prepared by the salt-leaching method with φ 300~500 μm pores (85-1 and 88-1) were tested for their capability to support cell growth for a wk. Cell growth in the scaffolds was attenuated until d 4 and then increased rapidly until d 7 post inoculation, except for scaffold 88-1, in which cell growth was relatively steady (Fig. 2a). Although cell growth in the 3050 scaffolds appeared to exceed that in the 1020 ones, the difference was not statistically significant. The growth of cells in the sponge-type scaffolds was ~1.5 to 3-fold higher than that in the 3050 nanofibrous scaffolds. Among the sponge-type scaffolds, the 88-1 scaffold supported cell growth better than the 85-1 scaffold did.

Osteoblastic differentiation of hBMSCs in the silk scaffolds was examined by treatment of ODM-1 followed by Alizarin S and von Kossa staining. Alizarin S and von Kossa staining demonstrated that treatment of ODM-1 induced differentiation of hBMSCs cultivated both on nanofibrous scaffolds (1020 and 3050) and sponge-type scaffolds (85-1 and 88-1; Fig. 2b). DAPI staining verified the presence of differentiated cells in scaffold 88-1 (Fig. 2c). Thus, all of the silk scaffolds tested could support growth and osteoblastic differentiation of hBMSCs in vitro.

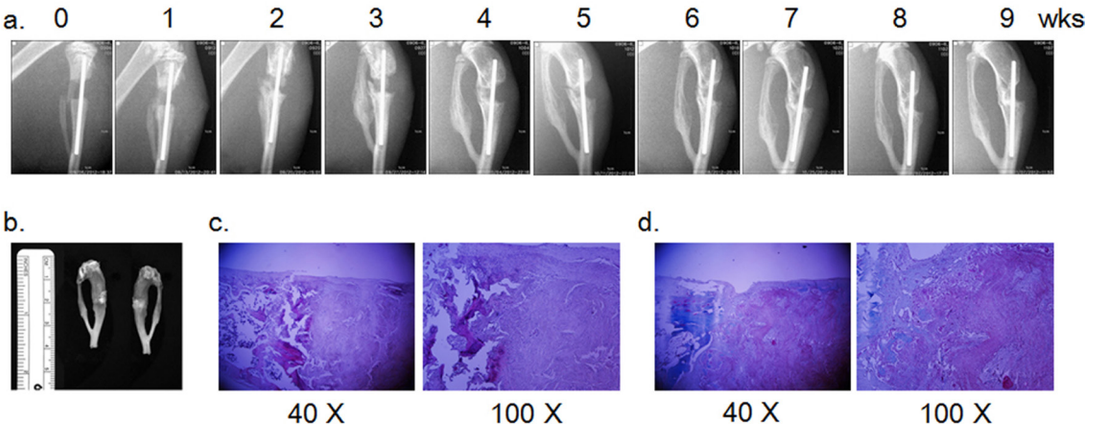

Fig. 3. Bone forming activity of a silk 3-D scaffold in the rat tibia diaphysis defect model. **a.** Weekly post-operation follow up by radiography. A nanofibrous silk scaffold (3050) was implanted into a 3-mm tibia diaphysis defect by intramedullary nailing (φ 0.9 mm). Callus formation and bone formation was monitored by X-ray imaging weekly from the day of operation (wk 0). **b.** Crus skeleton with implanted silk scaffold extirpated nine wk after surgery. **c.** H & E staining of a longitudinal section of the silk scaffold in the tibia diaphysis defect. **d.** Masson trichrome staining of a longitudinal section of the silk scaffold in the tibia diaphysis defect.

In vivo bone reconstitution capacity of silk 3-D scaffolds

Since a nanofibrous silk scaffold supports calvaria bone regrowth, bone forming activity of the 3050 nanofibrous scaffold was examined in a long bone defect model of rat tibia diaphysis (Park *et al*., 2010). Intramedullary nailing was employed to fix the silk scaffold in the tibia defect of rat hind limb. Although silk-filled gaps were shrunken by ~1 mm and dorsal contact with the tibia by the forward bending of broken bone displaced the silk scaffold ventrally 1 wk post operation, the position of the silk scaffold was maintained up to 9 wk after that point (Fig. 3a). Weekly monitoring of bone formation by X-ray imaging showed that opaqueness in the nanofibrous silk scaffolds did not increase with time. Lower limbs recovered from operated animals after 9 wk had silk scaffold protruding from the implanted site and reunion of the bone at dorsal region by the forward bending (Fig. 3b). H & E staining of the recovered tibia revealed new bone formation only at the boundary between implanted silk and undisturbed bone, although most of the silk scaffold remained intact (Fig. 3c and d). Formation of the bone tissue at the edge was also apparent from Masson trichrome staining (Fig. 3d). However, new bone formation within the silk scaffold was not observed even after 9 wk post operation. Remaining silk scaffolds were fragmented and infiltrated with histiocytes and multinucleate giant cells, signifying foreign body reaction (Fig. 3c). Masson trichrome stain visualized stream-like collagen within the silk scaffold deposited probably by percolated fibroblasts (Fig. 3d). Although new bone formation was evident at the edge of the silk scaffold, the implanted nanofibrous silk scaffold alone did not support bone ingrowth in the long bone defect model effectively.

Discussion

MSCs established from various sources, including bone marrow, dental pulp, adipose tissue, peripheral blood, and umbilical cord blood have the potential to differentiate into osteoblasts with appropriate treatments (Gamie *et al*., 2012). In this study, hBMSCs were induced to differentiate into osteoblasts by three different combinations of DEX, AA, and βG, with or without BMP-2. Although all three ODM increased ALP activity by a similar extent, Alizarin S and von Kossa staining showed that BMP-2-containing ODM-2 was significantly less efficient than ODM-1 and ODM-3 in mineral deposition. Inefficient mineral deposition in ODM-2-treated cells might be ascribed to BMP-2 because subtle difference in concentrations of DEX, AA, and βG in ODM-1 and ODM-3 did not make a significant difference in mineral deposition.

Attachment, growth, and differentiation of MSCs in 3-D scaffolds are required to produce bone tissue in vitro and to

reconstitute bone tissue in vivo (Murphy *et al*., 2013). Both nanofibrous and sponge-type silk 3-D scaffolds supported cell growth and differentiation. Differentiation of MSCs inoculated on the 3-D scaffolds was similar among the scaffolds. However, direct comparison of cell growth capacity in the scaffolds showed that cell growth was significantly faster in sponge-type scaffolds than in the nanofibrous ones, although both nanofibrous and sponge-type silk scaffolds are reported to be suitable to support cell ingrowth (Kim *et al*., 2005; Park *et al*., 2010). Cell growth would depend on surface area, surface property, material exchange rate, and yet unidentified properties of a scaffold (Murphy *et al*., 2013). However, it is not clear which one(s) of them should be critical to make the difference in cell growth between the two types of scaffolds.

Although the nanofibrous scaffold 3050 supported growth and osteoblastic differentiation of inoculated MSCs in vitro, bone tissue formation was limited at the edge of the implanted 3050 scaffolds in the in vivo tibia diaphysis defect model. Unlike the long bone defect model, the nanofibrous scaffold served as a guide of bone regrowth in the rat calvaria defect model (Park *et al*., 2010). The calvaria differs from the tibia in the mechanism of bone formation, mechanical properties, resorption, and composition (van den Bos *et al*., 2008). In addition, scaffolds implanted in the calvarial defect were thin, stable, and not weight bearing, which should provide favorable condition in regeneration of the bone defect. In contrast, scaffolds in the tibial defect were 3-mm-thick and were exposed to continuous pressure, which might explain the poor regenerative capacity of the long bone defect with the scaffold. Although reconstitution of the long bone defect with composite scaffold of bone mineral and synthetic biomaterials has been reported occasionally, incorporation of MSCs and/or growth factors in guiding scaffolds has been demonstrated to enhance bone formation in vivo significantly (Berner *et al*., 2013; Kuzyk *et al*., 2010). It is possible that loading MSCs into the nanofibrous scaffold 3050 might be required to facilitate healing of the long bone defect.

Healing a bone fracture requires firm stabilization of the fracture throughout the healing process (Marsell and Einhorn, 2011). Large animals, including sheep, rabbit, pig, and dog, have been employed in segmental bone defect model of the long bone partly because steady fixation of the fracture can be achieved with intramedullary nailing and plaster casting (Cancedda *et al*., 2007). The utility of small animals such as mouse and rat in study of the long bone defect model, especially in the tibia model, is limited because of the lack of suitable fixation measures (Histing *et al*., 2011). Although intramedullary nailing is widely used to stabilize bone fractures in humans and large animals, its utility in the rat tibia model has recently been reevaluated as an alternative of external fixation (Sigurdsen *et al*., 2009). Intramedullary nailing was applied to stabilize osteotomized tibia in this study and resulted in minor longitudinal shrinkage of defect and ventral curvature. However, direct application of straight intramedullary nail in the tibia model could maintain the defect location after the first wk of initial displacement. Shrinkage along the defect length might be ascribed to the repositioning of the nail toward the wide proximal region. Improved procedures such as locking the proximal region of the nail by a pin or a screw might be required to fix the nail in the desired position

In summary, the current study demonstrates that BMP-2-containing ODM (ODM-2) is less effective for promoting differentiation-associated mineral deposition of human MSCs than BMP-2-deficient media. Although silk scaffolds—both in the nanofibrous and sponge form—support growth and differentiation of MSCs in vitro, a nanofibrous silk scaffold by itself is not sufficient to reconstitute tibial defect in the rat hind limb. Since the nanofibrous scaffold is osteoconductive in the rat calvaria model and could sustain MSC ingrowth and differentiation in vitro (Park *et al*., 2010), MSC loading on implanting scaffold should improve bone-forming activity of the scaffold in the tibia defect model.

Acknowledgements

This work was supported by a grant from the Next Generation BioGreen 21 Program (No. PJ009051), Rural Development Administration, Republic of Korea.

References

Amini AR, Laurencin CT, Nukavarapu SP (2012) Bone tissue engineering: recent advances and challenges. Crit Rev Biomed Eng

40, 363-408.

Berner A, Reichert JC, Woodruff MA, Saifzadeh S, Morris AJ, Epari DR et al. (2013) Autologous vs. allogenic mesenchymal progenitor cells for the reconstruction of critical sized segmental tibial bone defects in aged sheep. Acta Biomater 9, 7874-7884.

Cancedda R, Giannoni P, Mastrogiacomo M (2007) A tissue engineering approach to bone repair in large animal models and in clinical practice. Biomaterials 28, 4240-4250.

Cao L, Liu G, Gan Y, Fan Q, Yang F, Zhang X et al. (2012) The use of autologous enriched bone marrow

MSCs to enhance osteoporotic bone defect repair in long-term estrogen deficient goats. Biomaterials 33, 5076-5084.

Dimarino AM, Caplan AI, Bonfield TL (2013) Mesenchymal stem cells in tissue repair. Front Immunol 4, 201.

Drosse I, Volkmer E, Capanna R, De Biase P, Mutschler W, Schieker M (2008) Tissue engineering for bone defect healing: an update on a multi-component approach. Injury 39 Suppl 2, S9-20.

Gamie Z, Tran GT, Vyzas G, Korres N, Heliotis M, Mantalaris A, Tsiridis E (2012) Stem cells combined with bone graft substitutes in skeletal tissue engineering. Expert Opin Biol Ther 12, 713-729.

Histing T, Garcia P, Holstein JH, Klein M, Matthys R, Nuetzi R et al. (2011) Small animal bone healing models: standards, tips, and pitfalls results of a consensus meeting. Bone 49, 591-599.

Hofmann S, Hilbe M, Fajardo RJ, Hagenmuller H, Nuss K, Arras M et al (2013) Remodeling of tissue- engineered bone structures in vivo. Eur J Pharm Biopharm 85, 119-129.

Huynh KM, Soh JW, Dash R, Sarkar D, Fisher PB, Kang D (2011) FOXM1 expression mediates growth suppression during terminal differentiation of HO-1 human metastatic melanoma cells. J Cell Physiol 226, 194-204.

Kasoju N, Bora U (2012) Silk fibroin in tissue engineering. Adv Healthc Mater 1, 393-412.

Ki CS, Park SY, Kim HJ, Jung HM, Woo KM, Lee JW et al (2008) Development of 3-D nanofibrous fibroin scaffold with high porosity by electrospinning: implications for bone regeneration. Biotechnol Lett 30, 405-410.

Kim HJ, Kim UJ, Kim HS, Li C, Wada M, Leisk GG et al. (2008) Bone tissue engineering with premineralized silk scaffolds. Bone 42, 1226-1234.

Kim HJ, Kim UJ, Vunjak-Novakovic G, Min BH, Kaplan DL (2005) Influence of macroporous protein scaffolds on bone tissue engineering from bone marrow stem cells. Biomaterials 26, 4442-4452.

Kim NR, Lee DH, Chung PH, Yang HC (2009) Distinct differentiation properties of human dental pulp cells on collagen, gelatin, and chitosan scaffolds. Oral Surg Oral Med Oral Pathol Oral Radiol Endod 108, e94-100.

Kirker-Head C, Karageorgiou V, Hofmann S, Fajardo R, Betz O, Merkle HP et al. (2007) BMP-silk composite matrices heal critically sized femoral defects. Bone 41, 247-255.

Kuzyk PR, Schemitsch EH, Davies JE (2010) A biodegradable scaffold for the treatment of a diaphyseal bone defect of the tibia. J Orthop Res 28, 474-480.

Kweon H, Lee KG, Chae CH, Balazsi C, Min SK, Kim JY et al. (2011) Development of nano- hydroxyapatite graft with silk fibroin scaffold as a new bone substitute. J Oral Maxillofac Surg 69, 1578-1586.

Marsell R, Einhorn TA (2011) The biology of fracture healing. Injury 42, 551-555.

Meinel L, Fajardo R, Hofmann S, Langer R, Chen J, Snyder B et al. (2005) Silk implants for the healing of critical size bone defects. Bone 37, 688-698.

Murphy CM, O'Brien FJ, Little DG, Schindeler A (2013) Cell-scaffold interactions in the bone tissue engineering triad. Eur Cell Mater 26, 120-132.

Park SY, Ki CS, Park YH, Jung HM, Woo KM, Kim HJ (2010) Electrospun silk fibroin scaffolds with macropores for bone regeneration: an in vitro and in vivo study. Tissue Eng Part A 16, 1271-1279.

Pittenger MF, Mackay AM, Beck SC, Jaiswal RK, Douglas R, Mosca JD et al. (1999) Multilineage potential of adult human mesenchymal stem cells. Science 284, 143-147.

Schroeder JE, Mosheiff R (2011) Tissue engineering approaches for bone repair: concepts and evidence. Injury 42, 609-613.

Sigurdsen UE, Reikeras O, Utvag SE (2009) External fixation compared to intramedullary nailing of tibial fractures in the rat. Acta Orthop 80, 375-379.

van den Bos T, Speijer D, Bank RA, Bromme D, Everts V (2008) Differences in matrix composition between calvaria and long bone in mice suggest differences in biomechanical properties and resorption: Special emphasis on collagen. Bone 43, 459-468.

Vepari C, Kaplan DL (2007) Silk as a Biomaterial. Prog Polym Sci 32, 991-1007.

Wang X, Wang Y, Gou W, Lu Q, Peng J, Lu S (2013) Role of mesenchymal stem cells in bone regeneration and fracture repair: a review. Int Orthop.

Wang Y, Kim HJ, Vunjak-Novakovic G, Kaplan DL (2006) Stem cell-based tissue engineering with silk biomaterials. Biomaterials 27,

6064-6082.

Wolfe M, Pochampally R, Swaney W, Reger RL (2008) Isolation and culture of bone marrow-derived human multipotent stromal cells (hMSCs). Methods Mol Biol 449, 3-25.

Zhang Y, Fan W, Ma Z, Wu C, Fang W, Liu G et al. (2010) The effects of pore architecture in silk fibroin scaffolds on the growth and differentiation of mesenchymal stem cells expressing BMP7. Acta Biomater 6, 3021-3028.

Zimmermann G, Moghaddam A (2011) Allograft bone matrix versus synthetic bone graft substitutes. Injury 42 Suppl 2, S16-21.